Radiation and Mass Transfer Effects on MHD Natural Convection Flow over an Inclined Plate

R.L.V.Renuka Devi[1], T.Poornima[2], N. Bhaskar Reddy[3], S.Venkataramana[4]
[1,2,3,4]*Department of Mathematics, Sri Venkateswara University, Tirupati, India*

ABSTRACT: *A numerical solution for the unsteady, natural convective flow of heat and mass transfer along an inclined plate is presented. The dimensionless unsteady, coupled, and non-linear partial differential conservation equations for the boundary layer regime are solved by an efficient, accurate and unconditionally stable finite difference scheme of the Crank-Nicolson type. The velocity, temperature, and concentration fields have been studied for the effect of Magnetic parameter, buoyancy ratio parameter, Prandtl number, radiation parameter and Schmidt number. The local skin-friction, Nusselt number and Sherwood number are also presented and analyzed graphically.*

Keywords*: Unsteady flow, Inclined plate, Finite difference method, Radiation, Mass transfer.*

I. INTRODUCTION

The buoyancy force induced by density differences in a fluid cause's natural convection. Natural convection flows are frequently encountered in physics and engineering problems such as chemical catalytic reactors, nuclear waste material etc. Transient free convection is important in many practical applications such as thermal regulation process, security of energy systems etc. In literature, extensive research work has been performed to examine the effect of natural convection on flow past a plate. The first attempt in this direction was made by Callahan and Marner [1] who solved the non-linear system of equations by explicit finite difference scheme, which is not always convergent. Soundalgekar and Ganesan [2] studied the same problem by implicit finite difference scheme which is always stable and convergent. Recently, finite difference solution of natural convection flow over a heated plate with different inclination was studied by Begum et al. [3].

Two dimensional natural convection heat and mass transfer flow past a semi-infinite flat plate has been receiving the attention of many researchers because of its wide applications in industry and technological fields. Natural convection along an inclined plate has received less attention than the case of vertical and horizontal plates. Finite-difference technique has been used in natural convective flow analysis by many researchers. Callahan and Marner [4] have presented a paper on transient free convection with mass transfer effects and to solve the problem by explicit finite difference technique. Soundalgekar and Ganesan [5] solved the same problem using implicit finite difference technique and compared the result with those of Marner and Callahan [6] and both the results agree well. Chamkha et al. [7] presented similarity solutions for hydromagnetic simultaneous heat and mass transfer by natural convection from inclined plate with thermal heat generation or absorption employing implicit finite difference technique. Ganesan and Palani [8] studied free convection effects on the flow of water at 4ºC past a semi-infinite inclined flat plate and solved the problem using implicit finite difference technique.

Magnetohydrodynamic flows have applications in meteorology, solar physics, cosmic fluid dynamics, astrophysics, geophysics and in the motion of earth's core. In addition from the technological point of view, MHD free convection flows have significant applications in the field of stellar and planetary magnetospheres, aeronautical plasma flows, chemical engineering and electronics. An excellent summary of applications is to be found in Hughes and Young [9]. Raptis [10] studied mathematically the case of time varying two dimensional natural convective flow of an incompressible, electrically conducting fluid along an infinite vertical porous plate embedded in a porous medium. Helmy [11] studied MHD unsteady free convection flow past a vertical porous plate embedded in a porous medium. Elbashbeshy [12] studied heat and mass transfer along a vertical plate in the presence of magnetic field.

In the context of space technology and in the processes involving high temperatures, the effects of radiation are of vital importance. Recent developments in hypersonic flights, missile re-entry, rocket combustion chambers, power plants for inter planetary flight and gas cooled nuclear reactors, have focused attention on thermal radiation as a mode of energy transfer, and emphasized the need for improved understanding of radiative transfer in these processes. Cess [13] presented radiation effects on the boundary layer flow of an absorbing fluid past a vertical plate, by using the Rosseland diffusion model. Several authors have also studied thermal radiating MHD boundary layer flows with applications in astrophysical fluid dynamics. Mosa [14] discussed one of the first models for combined radiative hydromagnetic heat transfer,

considering the case of free convective channel flows with an axial temperature gradient. Nath et al. [15] obtained a set of similarity solutions for radiative-MHD stellar point explosion dynamics using shooting method. Takhar et al. [16] studied radiation effects on MHD free convection flow past a semi infinite vertical plate where the viscosity and thermal conductivity were assumed constant. Azzam [17] studied radiation effects on the MHD mixed convective flow past a semi infinite moving vertical plate for the case of high temperature differences.

However, the interaction of natural convection flow of an electrically conducting fluid past an inclined plate in the presence of radiation and mass transfer has received little attention. Hence, in the present chapter an attempt is made to analyze the mass transfer effects on MHD natural convection flow along a heated inclined semi-infinite plate in the presence of radiation. The equations of continuity, linear momentum, energy and diffusion, which govern the flow field, are solved by an implicit finite difference method of Crank-Nicolson type. The behavior of the velocity, temperature, concentration, skin-friction, Nusselt number and Sherwood number has been discussed for variations in the physical parameters.

II. MATHEMATICAL ANALYSIS

An unsteady two-dimensional natural convection flow of a viscous, incompressible, electrically conducting, radiating fluid past a heated inclined semi infinite plate is considered. The fluid is assumed to be gray, absorbing-emitting but non-scattering. The x-axis is taken along the plate and the y-axis normal to it. Initially, it is assumed that the plate and the fluid are at the same temperature T'_∞ and concentration level C'_∞ everywhere in the fluid. At time t>0, the temperature of the plate and the concentration level near the plate are raised to T'_w and C'_w respectively and are maintained constantly thereafter. A uniform magnetic field is applied in the direction perpendicular to the plate and that the induced magnetic field is neglected. The transverse applied magnetic field and magnetic Reynolds number are assumed to be very small, so that the induced magnetic field is negligible. It is assumed that the concentration *C′* of the diffusing species in the binary mixture is very less in comparison to the other chemical species, which are present, and hence the Soret and Dufour effects are negligible. It is also assumed that there is no chemical reaction between the diffusing species and the fluid. Then, under the above assumptions, in the absence of an input electric field, the governing boundary layer equations with Boussinesq's approximation are

$$\frac{\partial u}{\partial x}+\frac{\partial v}{\partial y}=0 \tag{1}$$

$$\frac{\partial u}{\partial t'}+u\frac{\partial u}{\partial x}+v\frac{\partial u}{\partial y}=g\beta(T-T_\infty)\sin\alpha+g\beta^*(C-C_\infty)\sin\alpha+\nu\frac{\partial^2 u}{\partial y^2}-\frac{\sigma B_0^2}{\rho}u \tag{2}$$

$$\frac{\partial T'}{\partial t'}+u\frac{\partial T'}{\partial x}+v\frac{\partial T'}{\partial y}=\alpha\frac{\partial^2 T'}{\partial y}-\frac{1}{\rho c_p}\frac{\partial q_r}{\partial y} \tag{3}$$

$$\frac{\partial C'}{\partial t'}+u\frac{\partial C'}{\partial x}+v\frac{\partial C'}{\partial y}=D\frac{\partial^2 C'}{\partial y^2} \tag{4}$$

The initial and boundary conditions are

$$t'\le 0: u=0, v=0, T'=T'_\infty, C'=C'_\infty \; t'>0: u=0, v=0, T'=T'_w, C'=C'_w \; at \; y=0$$

$$u=0, T'=T'_\infty, C'=C'_\infty \; at \;\; x=0$$

$$u\to 0, T'\to T'_\infty, C'\to C'_\infty \; \textbf{as} \;\; y\to\infty \tag{5}$$

Where u, v are the velocity components in x, y directions respectively, t' - the time, g - the acceleration due to gravity, β- the volumetric coefficient of thermal expansion, β^* - the volumetric coefficient of expansion with concentration, T - the temperature of the fluid in the boundary layer, C - the species concentration in the boundary layer, ν- the kinematic viscosity, T_w' - the wall temperature, T_∞' - the free stream temperature far away from the plate, C_w' - the concentration at the plate, C_∞' - the free stream concentration far away from the plate, σ- the electrical conductivity, B_0 - the magnetic induction, ρ- the density of the fluid, α- the thermal diffusivity, c_p - the specific heat at constant pressure, q_r - the radiation heat flux and D - the species diffusion coefficient.

The second term on the right hand side of equation (2.3) represents the radiative heat flux; Thermal radiation is assumed to be present in the form of a unidirectional flux in the y-direction i.e., q_r (transverse to the surface).

By using the Rosseland approximation (Brewster [18]), the radiative heat flux q_r is given by

$$q_r = -\frac{4\sigma_s}{3k_e}\frac{\partial T'^4}{\partial y} \tag{6}$$

Where σ_s is the Stefan-Boltzmann constant and k_e - the mean absorption coefficient. It should be noted that by using the Rosseland approximation, the present analysis is limited to optically thick fluids. If the temperature differences within the flow are sufficiently small, then Equation (2.6) can be linearized by expanding T'^4 into the Taylor series about T'_∞, which after neglecting higher order terms takes the form

$$T'^4 \cong 4T'^3_\infty T' - 3T'^4_\infty \tag{7}$$

In view of equations (2.6) and (2.7), equation (2.3) reduces to

$$\frac{\partial T'}{\partial t'} + u\frac{\partial T'}{\partial x} + v\frac{\partial T'}{\partial y} = \alpha\frac{\partial^2 T'}{\partial y^2} + \frac{16\sigma_s T'^3_\infty}{3k_e\rho c_p}\frac{\partial^2 T'}{\partial y^2} \tag{8}$$

From the technological point of view, for the type of problem under conditions, the coefficient of skin-friction, heat and mass transfer are important.

Local and average skin-frictions are given respectively by

$$\tau'_x = -\mu\left(\frac{\partial u}{\partial y}\right)_{y=0} \tag{9}$$

$$\bar{\tau}_L = \frac{-1}{L}\int_0^L \mu\left(\frac{\partial u}{\partial y}\right)_{y=0} dx \tag{10}$$

Local and average Nusselt numbers are given respectively by

$$Nu_x = \frac{-x\left(\frac{\partial T'}{\partial y}\right)_{y=0}}{T'_w - T'_\infty} \tag{11}$$

$$\overline{Nu}_L = -\int_0^L \left[\left(\frac{\partial T'}{\partial y}\right)_{y=0} \Big/ (T'_w - T'_\infty)\right] dx \tag{12}$$

Local and average Sherwood numbers are given respectively by

$$Sh_x = \frac{-x\left(\frac{\partial C'}{\partial y}\right)_{y=0}}{C'_w - C'_\infty} \tag{13}$$

$$\overline{Sh}_L = -\int_0^L \left[\left(\frac{\partial C'}{\partial y}\right)_{y=0} \Big/ (C'_w - C'_\infty)\right] dx \tag{14}$$

In order to write the governing equations and the boundary conditions in dimensionless form, the following non-dimensional quantities are introduced**.**

$$X = \frac{x}{L},\quad Y = \frac{yGr^{1/4}}{L},\quad t' = \frac{L^2}{\nu}Gr^{-1/2},\quad U = \frac{uLGr^{-1/2}}{\nu},\quad V = \frac{vLGr^{-1/4}}{\nu}, Gr = \frac{g\beta L^3(T'_w - T'_\infty)}{\nu^2}, Gc = \frac{g\beta^* L^3(C'_w - C'_\infty)}{\nu^2}$$

$$T = \frac{T' - T'_\infty}{T'_w - T'_\infty}, C = \frac{C' - C'_\infty}{C'_w - C'_\infty}, M = \frac{\sigma B_0^2 \nu}{L^2}, \Pr = \frac{\nu}{\alpha},\quad Sc = \frac{\nu}{D}, N = \frac{\beta^*(C'_w - C'_\infty)}{\beta(T'_w - T'_\infty)}, F = \frac{k_e k}{4\sigma_s T_\infty^3} \tag{15}$$

where L is the characteristic length of the plate and k-the thermal conductivity.

In view of (2.15), the equations (1), (2), (8) and (4) are reduced to the following non-dimensional form

$$\frac{\partial U}{\partial X} + \frac{\partial V}{\partial Y} = 0 \tag{16}$$

$$\frac{\partial U}{\partial t} + U\frac{\partial U}{\partial X} + V\frac{\partial U}{\partial Y} = \frac{\partial^2 U}{\partial Y^2} + (T + NC)\sin\alpha - MU \tag{17}$$

$$\frac{\partial T}{\partial t}+U\frac{\partial T}{\partial X}+V\frac{\partial T}{\partial Y}=\frac{1}{\Pr}\left(1+\frac{4}{3F}\right)\frac{\partial^2 T}{\partial Y^2} \tag{18}$$

$$\frac{\partial C}{\partial t}+U\frac{\partial C}{\partial X}+V\frac{\partial C}{\partial Y}=\frac{1}{Sc}\frac{\partial^2 C}{\partial Y^2} \tag{19}$$

where, *Gr*, *M*, *F*, *Pr*, *N* and *Sc* are thermal Grashof number, radiation parameter, Prandtl number, buoyancy ratio parameter and Schmidt number respectively.

The corresponding initial and boundary conditions are

$$\begin{aligned} &t\le 0: U=0, V=0, T=0, C=0 \\ &t>0: U=0, V=0, T=1, C=1 \quad at \quad Y=0 \\ &\quad U=0, V=0, T=0, C=0 \ \ at \ \ X=0 \\ &\quad U\to 0, T\to 0, C\to 0 \ \ as\ Y\to\infty \end{aligned} \tag{20}$$

Local and average skin-frictions in non-dimensional form are

$$\tau_x' = Gr^{3/4}\left(\frac{\partial u}{\partial y}\right)_{y=0} \tag{21}$$

$$\bar{\tau} = Gr^{3/4}\int_0^1 \left(\frac{\partial u}{\partial y}\right)_{y=0} dX \tag{22}$$

Local and average Nusselt numbers in non-dimensional form are

$$Nu_x = -XGr^{1/4}\left(\frac{\partial T}{\partial Y}\right)_{y=0} \tag{23}$$

$$\overline{Nu} = -Gr^{1/4}\int_0^1 \left(\frac{\partial T}{\partial Y}\right)_{y=0} dX \tag{24}$$

Local and average Sherwood numbers in non-dimensional form are

$$Sh_x = -XGr^{1/4}\left(\frac{\partial C}{\partial Y}\right)_{y=0} \tag{25}$$

$$\overline{Sh} = -Gr^{1/4}\int_0^1 \left(\frac{\partial C}{\partial Y}\right)_{y=0} dX \tag{26}$$

III. METHOD OF SOLUTION

In order to solve the unsteady, non-linear, coupled equations (16) - (19), under the boundary conditions (20), an implicit finite difference scheme of Crank-Nicholson type has been employed. The region of integration is considered as a rectangle with sides $X_{\max}$(=1) and $Y_{\max}$ (=14), where $Y_{\max}$ corresponds to $Y=\infty$, which lies very well outside the momentum, energy and concentration boundary layers. The maximum value of *Y* was chosen as 14 after some preliminary investigations so that the last two of the boundary conditions of equation (20) are satisfied with in the tolerance limit 10^{-5}. The grid system is shown in the following figure A**.**

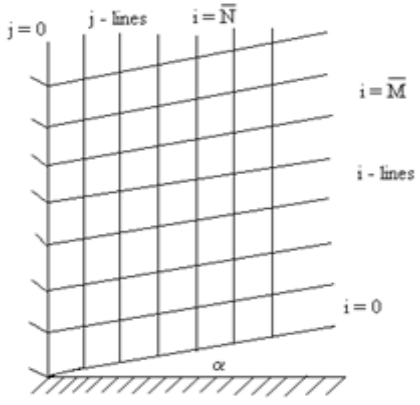

Figure A: Grid system

The finite difference equations corresponding to equations (16) - (19) are as follows

$$\frac{\left[U_{i,j}^{n+1}-U_{i-1,j}^{n+1}+U_{i,j}^{n}-U_{i-1,j}^{n}+U_{i,j-1}^{n+1}-U_{i-1,j-1}^{n+1}+U_{i,j-1}^{n}-U_{i-1,j-1}^{n}\right]}{4\Delta X}+\frac{\left[V_{i,j}^{n+1}-V_{i,j-1}^{n+1}+V_{i,j}^{n}-V_{i,j-1}^{n}\right]}{2\Delta Y}=0 \tag{27}$$

$$\frac{\left[U_{i,j}^{n+1}-U_{i,j}^{n}\right]}{\Delta t}+U_{i,j}^{n}\frac{\left[U_{i,j}^{n+1}-U_{i-1,j}^{n+1}+U_{i,j}^{n}-U_{i-1,j}^{n}\right]}{2\Delta X}+V_{i,j}^{n}\frac{\left[U_{i,j+1}^{n+1}-U_{i,j-1}^{n+1}+U_{i,j+1}^{n}-U_{i,j-1}^{n}\right]}{4\Delta Y}=$$
$$\left(\frac{\left[T_{i,j}^{n+1}+T_{i,j}^{n}\right]}{2}+N\frac{\left[C_{i,j}^{n+1}+C_{i,j}^{n}\right]}{2}\right)\sin\alpha+\frac{\left[U_{i,j-1}^{n+1}-2\ U_{i,j}^{n+1}+U_{i,j+1}^{n+1}+U_{i,j-1}^{n}-2U_{i,j}^{n}+U_{i,j+1}^{n}\right]}{2(\Delta Y)^{2}}-M\frac{\left[U_{i,j}^{n+1}+U_{i,j}^{n}\right]}{2} \tag{28}$$

$$\frac{[T_{i,j}^{n+1}-T_{i,j}^{n}]}{\Delta t}+U_{i,j}^{n}\frac{\left[T_{i,j}^{n+1}-T_{i-1,j}^{n+1}+T_{i,j}^{n}-T_{i-1,j}^{n}\right]}{2\Delta X}+V_{i,j}^{n}\frac{\left[T_{i,j+1}^{n+1}-T_{i,j-1}^{n+1}+T_{i,j+1}^{n}-T_{i,j-1}^{n}\right]}{4\Delta Y}=$$
$$\frac{1}{\Pr}\left(1+\frac{4}{3F}\right)\frac{\left[T_{i,j-1}^{n+1}-2T_{i,j}^{n+1}+T_{i,j+1}^{n+1}+T_{i,j-1}^{n}-2T_{i,j}^{n}+T_{i,j+1}^{n}\right]}{2(\Delta Y)^{2}} \tag{29}$$

$$\frac{\left[C_{i,j}^{n+1}-C_{i,j}^{n}\right]}{\Delta t}+U_{i,j}^{n}\frac{\left[C_{i,j}^{n+1}-C_{i-1,j}^{n+1}+C_{i,j}^{n}-C_{i-1,j}^{n}\right]}{2\Delta X}+V_{i,j}^{n}\frac{\left[C_{i,j+1}^{n+1}-C_{i,j-1}^{n+1}+C_{i,j+1}^{n}-C_{i,j-1}^{n}\right]}{4\Delta Y}=$$
$$\frac{1}{Sc}\frac{\left[C_{i,j-1}^{n+1}-2\ C_{i,j}^{n+1}+C_{i,j+1}^{n+1}+C_{i,j-1}^{n}-2C_{i,j}^{n}+C_{i,j+1}^{n}\right]}{2(\Delta Y)^{2}} \tag{30}$$

Here, the subscript *i*-designates the grid point along the X-direction, *j*-along the Y-direction and the superscript *n* along the *t*-direction. An appropriate mesh size considered for the calculation is ΔX = 0.018, ΔY = 0.25,and the time step $\Delta t = 0.01$.During any one time step, the coefficients $U_{i.j}^{n}$ and $V_{i.j}^{n}$ appearing in the difference equations are treated as constants. The values of *C, T, U* and *V* at time level (*n+1*) using the known values at previous time level (*n*) are calculated as follows.

The finite difference equation (30) at every internal nodal point on a particular *i*-level constitute a tridiagonal system of equations. Such a system of equations is solved by using Thomas algorithm as discussed in Carnahan et al. [33]. Thus, the values of *C* are known at every internal nodal point on a particular *i* at $(n+1)^{th}$ time level. Similarly, the values of *T* are calculated from the equation (29). Using the values of *C* and *T* at $(n+1)^{th}$ time level in the equation (28), the values of *U* at $(n+1)^{th}$ time level are found in similar manner. Thus the values of *C, T* and *U* are known on a particular i-level. Then the values of *V* are calculated explicitly using the equation (27) at every nodal point at particular *i*-level at $(n+1)^{th}$ time level. This process is repeated for various *i*-levels. Thus the values of C, T, U and V are known, at all grid points in the rectangular region at $(n+1)^{th}$ time level.

Computations are carried out until the steady state is reached. The steady-state solution is assumed to have been reached, when the absolute difference between the values of *U* as well as temperature *T* and concentration *C* at two consecutive time steps are less than 10^{-5} at all grid points.

The derivatives involved in the equations (21) - (26) are evaluated using five-point approximation formula and then the integrals are evaluated using Newton-Cotes closed integration formula.

IV. STABILITY OF THE SCHEME

In this section, the stability of the finite difference equations has been discussed using the well-known Von-Neumann technique. This method introduces an initial error represented by a finite Fourier series and examines how this error propagates during the solution. The general terms of the Fourier expansion for *U, T* and *C* at a time arbitrarily called t = 0 are assumed to be of the form $e^{i\varphi x}\ e^{i\phi y}$ (here i = $\sqrt{-1}$). At a later time *t*, these terms will become

$$\begin{aligned} U &= F(t)\ e^{i\varphi x}e^{i\phi y} \\ T &= G(t)\ e^{i\varphi x}e^{i\phi y} \\ C &= H(t)\ e^{i\varphi x}e^{i\phi y} \end{aligned} \tag{4.1}$$

Substituting (4.1) in the equations (27) – (30) under the assumption that the coefficients *U* and *V* are constants over any one time step and denoting the values after on time step by $F', G' \text{ and } H'$, one may get after simplification.

$$\frac{(F'-F)}{\Delta t}+U\frac{(F'+F)\ \ (1-e^{-i\varphi\Delta X})}{2\Delta X}+V\frac{(F'+F)\ \ i\sin(\phi\Delta Y)}{2\Delta Y}=$$
$$\left[\frac{(G'+G)}{2}+N\frac{(H+H')}{2}\right]\sin\alpha+\frac{(F'+F)\ \ (\cos\phi\Delta Y-1)}{(\Delta Y)^2} \quad (4.2)$$

$$\frac{(G'-G)}{\Delta t}+U\frac{(G'+G)\ \ (1-e^{-i\varphi\Delta X})}{2\Delta X}+V\frac{(G'+G)\ \ i\sin(\phi\Delta Y)}{2\Delta Y}=$$
$$\left(1+\frac{4}{3F}\right)\frac{(G'+G)\ \ (\cos\phi\Delta Y-1)}{\Pr(\Delta Y)^2} \quad (4.3)$$

$$\frac{(H'-H)}{\Delta t}+U\frac{(H'+H)\ \ (1-e^{-i\varphi\Delta X})}{2\Delta X}+V\frac{(H'+H)\ \ i\sin(\phi\Delta Y)}{2\Delta Y}=$$
$$\frac{(H'+H)\ \ (\cos\phi\Delta Y-1)}{Sc(\Delta Y)^2} \quad (4.4)$$

Equations (4.2) – (4.4) can be written as

$$(1+A)F'=(1-A)F+\frac{\Delta t}{2}\left[(G'+G)+N(H'+H)\right]Sin\alpha \quad (4.5)$$

(1+B) G' = (1-B)G (4.6)

(1+E) H' = (1-E)H (4.7)

where

$$A=\frac{U}{2}\frac{\Delta t}{\Delta X}(1-e^{-i\varphi\Delta X})+\frac{V}{2}\frac{\Delta t}{\Delta Y}i\sin(\phi\Delta Y)\quad B=\frac{U}{2}\frac{\Delta t}{\Delta X}(1-e^{-i\varphi\Delta X})+\frac{V}{2}\frac{\Delta t}{\Delta Y}i\sin(\phi\Delta Y)$$
$$-(\cos\phi\Delta Y-1)\frac{\Delta t}{(\Delta Y)^2}\qquad -(\cos\phi\Delta Y-1)\left(1+\frac{4}{3F}\right)\frac{\Delta t}{\Pr(\Delta Y)^2}$$
$$E=\frac{U}{2}\frac{\Delta t}{\Delta X}(1-e^{-i\varphi\Delta X})+\frac{V}{2}\frac{\Delta t}{\Delta Y}i\sin(\phi\Delta Y)$$
$$-(\cos\phi\Delta Y-1)\frac{\Delta t}{Sc(\Delta Y)^2}$$

After eliminating G' and H' in the equation (4.5) using the equations (4.6) and (4.7), the resultant equation and equations (4.6) and (4.7) can be written in matrix form as follows.

$$\begin{bmatrix}F'\\G'\\H'\end{bmatrix}=\begin{bmatrix}\frac{1-A}{1+A} & D_1 & D_2\\ 0 & \frac{1-B}{1+B} & 0\\ 0 & 0 & \frac{1-E}{1+E}\end{bmatrix}\begin{bmatrix}F\\G\\H\end{bmatrix} \quad (4.8)$$

where $D_1=\dfrac{\Delta t sin\alpha}{(1+A)(1+B)}$ and $D_2=\dfrac{\Delta t sin\alpha}{(1+A)(1+E)}$

Now, for the stability of the finite difference scheme, the modulus of each eigen value of the amplification matrix must not exceed unity. Since this matrix in the equation (4.8) is triangular, the eigen values are diagonal elements. Hence, the eigen values of the amplification matrix are *(1–A)/(1+A), (1–B)/(1+B)* and *(1–E)/(1+E).* Assuming that *U* is everywhere non-negative and *V* is everywhere non-positive we get

$$A = 2a\sin^2\left(\frac{\varphi\Delta X}{2}\right) + 2c\sin^2\left(\frac{\phi\Delta Y}{2}\right)$$
$$+i\left(a\sin\varphi\Delta X + b\sin\phi\Delta Y\right)$$
$$B = 2a\sin^2\left(\frac{\varphi\Delta X}{2}\right) + 2\left(1+\frac{4}{3F}\right)\frac{c}{\Pr}\sin^2\left(\frac{\phi\Delta Y}{2}\right)$$
$$+i\left(a\sin\varphi\Delta X + b\sin\phi\Delta Y\right)$$
$$A = 2a\sin^2\left(\frac{\varphi\Delta X}{2}\right) + \frac{2}{Sc}c\sin^2\left(\frac{\phi\Delta Y}{2}\right)$$
$$+i\left(a\sin\varphi\Delta X + b\sin\phi\Delta Y\right)$$

where

a = $\frac{U\Delta t}{2\Delta X}$, b = $\frac{|V|\Delta t}{2\Delta Y}$ and c = $\frac{\Delta t}{(\Delta Y)^2}$

Since the real part of A is greater than or equal to zero, $\left|(1-A)/(1+A)\right| \le 1$ always. Similarly, $\left|(1-B)/(1+B)\right| \le 1$ and $\left|(1-E)/(1+E)\right| \le 1$.

Hence, the scheme is unconditionally stable. The local truncation error is O($\Delta t^2 + \Delta Y^2 + \Delta X$) and it tends to zero as Δt, ΔY and ΔX tend to zero. Therefore the scheme is compatible. The stability and compatibility ensures convergence.

V. RESULTS AND DISCUSSION

The aim of present study is to investigate the effect of radiation and mass transfer on an unsteady free convection flow of a viscous incompressible electrically conducting fluid over an inclined heated plate. A representative set of numerical results is shown graphically in Figs.1-20, to illustrate the influence of physical parameters viz., radiation parameter *F*, buoyancy ratio parameter *N*, Prandtl number *Pr*, Schmidt number *Sc*, and magnetic parameter *M* on the velocity, temperature, concentration, skin-friction, Nusselt number and Sherwood number. Here the value of *Pr* is chosen as 0.72, which corresponds to air. The values of *Sc* are chosen such that they represent Helium (0.24), Ammonia (0.78). The other parameters are arbitrarily chosen.

In order to ascertain the accuracy of the numerical results, the present study is compared with the previous study. The velocity profiles of the present problem for *Sc* = 0.0, *Pr* = 0.72, *N* = 0.0, M=0.0, F=0.0, t=0.40, $\alpha=60^0$, *X* = 1.0 are compared with the available solution of Begum et al [3] in Fig.1. It is observed that the present results are in good agreement with that of Begum et al. [3] .

The effects of inclined angle α, on the transient velocity are displayed in Fig.2. It is noticed that the velocity increases with increasing values of the inclined angle. The effects of the magnetic parameter *M* on the transient velocity are illustrated in Fig.3. It is seen that, as expected, the velocity decreases with an increase in the magnetic parameter. The magnetic parameter is found to retard the velocity at all points of the flow field. It is because that the application of transverse magnetic field will result in a resistive type force (Lorentz force) similar to drag force which tends to resist the fluid flow and thus reducing its velocity. Also, the boundary layer thickness decreases with an increase in the magnetic parameter. The effect of *N*, on the transient velocity is displayed in Fig.4. It is noticed that the velocity increases with increasing values of the buoyancy ratio parameter. The effect of *F*, on the transient velocity is displayed in Fig.5. It can be seen that an increase in the thermal radiation parameter produces significant decreases in the velocity boundary layer.

The steady state temperature for different values of *M* is displayed in Fig.6. It can be seen that an increase in the magnetic parameter produces significant increases in the temperature boundary layer. Fig.7 shows the distribution of steady state temperature against Y for various *N* values. The profiles in Fig.7 attest that with an increase in *N* the thermal boundary layer will be decreased in thickness and there will be a corresponding uniformity of temperature distributions across the boundary layer. The effect of radiation parameter on the transient temperature can be observed from Fig.8. It can be seen that an increase in the radiation parameter leads to a decrease in the temperature.

Fig.9 shows the distribution of T against Y for various *Pr* values. The profiles in Fig.9 attest that with an increase in *Pr* the thermal boundary layer will be decreased in thickness and there will be a corresponding uniformity of temperature distributions across the boundary layer. It is observed that the maximum temperature

correspond to lower *Pr* values. The profiles also steepen and intersect the abscissa faster for higher *Pr* fluids i.e. temperatures across the boundary layer (normal to wall) reach zero faster.

The steady state concentration for the different values *M* is displayed in Fig.10. It can be seen that an increase in the magnetic parameter produces significant increase in the concentration boundary layer. The effect of *N*, on the steady state concentration is displayed in Fig.11. It is noticed that the concentration decreases with increasing values of the buoyancy ratio parameter. The effect of F, on the steady state concentration is represented in Fig.12. It is noticed that the concentration decreases with increasing values of the radiation parameter. Fig.13 shows the distribution of transient concentration against Y for various *Sc* values. The profiles in Fig.13 attest that with an increase in *Sc* the concentration boundary layer will be decreased in thickness and there will be a corresponding uniformity of concentration distributions across the boundary layer.

Fig.14 illustrates the effects of M, N and F on the local skin-friction. The local skin-friction is found to decrease due to an increase in the magnetic field strength. An increase in N or F produces an increase in the local skin-friction. The effects M, N and F on the average skin-friction are shown in Fig.15. It is observed that the average skin-friction increases as N or F increases, and it decreases as M increases. Figs.16 and 17 show the effect of Pr and F on the local and average Nusselt numbers respectively. It is observed that the local and average Nusselt numbers increase as Pr increases, and decrease as F increases. Figs.18, 19 and 20 display the effect of Sc and F on the local and average Sherwood numbers respectively. It can be observed that as Sc or F increases the local and average Sherwood numbers increase.

VI. CONCLUTIONS

An Unsteady two dimensional natural convection boundary layer flow of heat and mass transfer over heated plate with different inclinations in the presence of radiation has been studied. Implicit finite difference scheme of Crank-Nicolson type was employed to obtain the solution of the governing equations. The present solutions were validated by comparing with solutions existing in the literature. Our results show a good agreement with the existing work in the literature. The results are summarized as follows:

1. Magnetic field elevates the temperature and concentration, and reduces the velocity.
2. The angle of inclination enhances the velocity
3. The radiation enhances the velocity and temperature, and reduces the concentration.
4. The radiation enhances the local and average skin-friction, and local and average Sherwood number, and reduces the local and average Nusselt number.

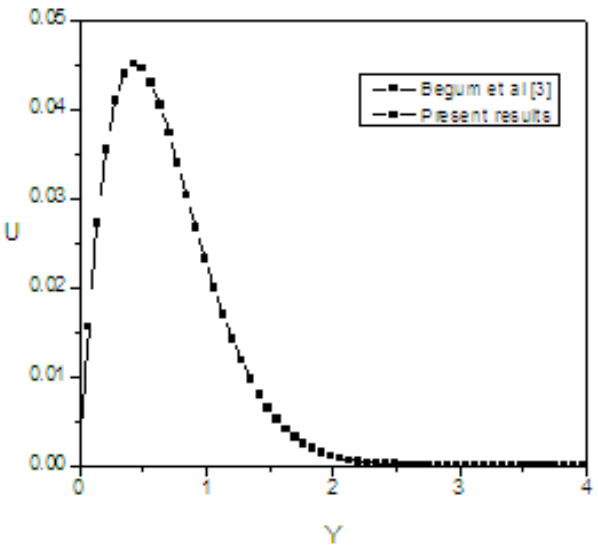

Fig. 1 Comparison of velocity for t=0.40, Pr=0.72 and $\alpha=60^0$

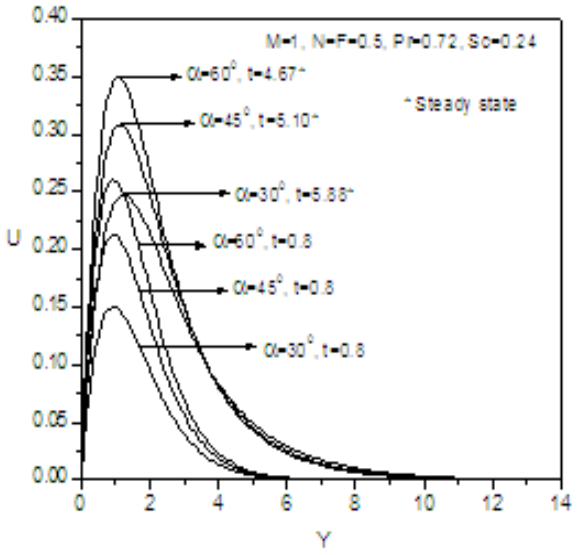

Fig 2 Transient velocity at X=1.0 for the different values of α.

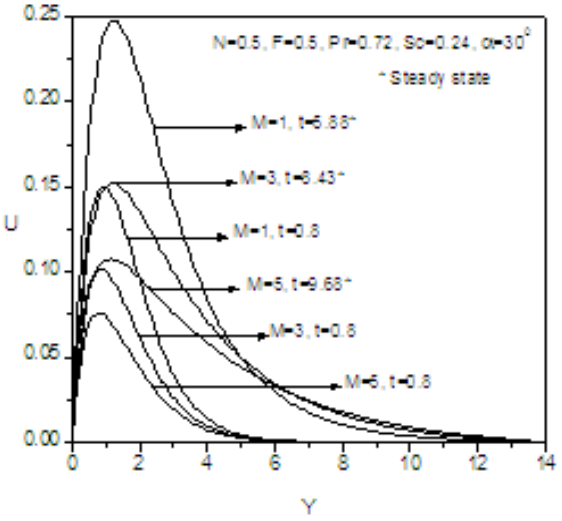

Fig 3 Transient velocity at X=1.0 for the different values of *M*.

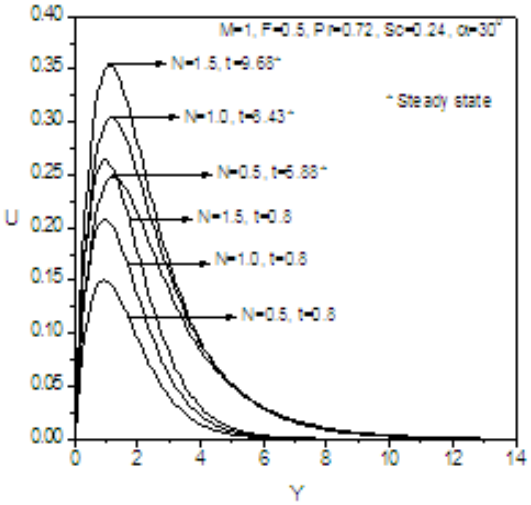

Fig 4 Transient velocity at X=1.0 for the different values of *N*.

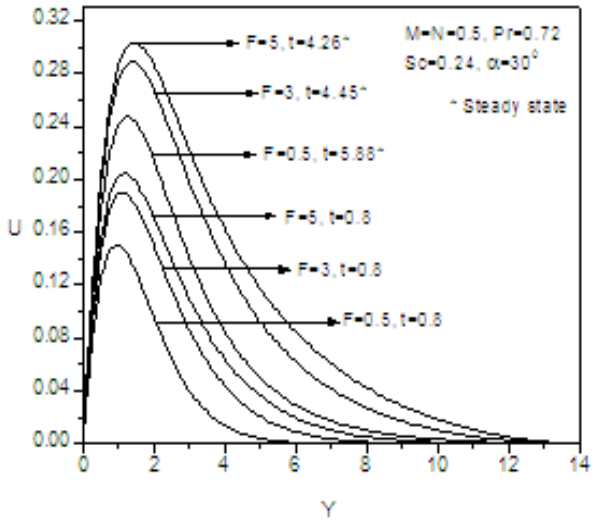

Fig 5 Transient velocity for at X=1.0 the different values of *F*.

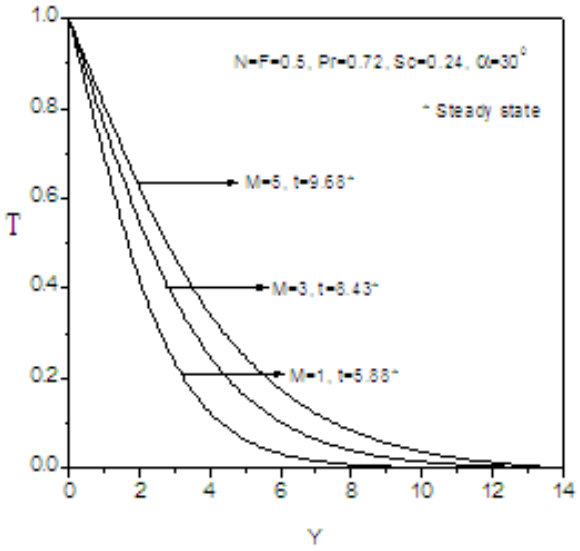

Fig 6 Steady state temperature for different values of *M* at X=1.0.

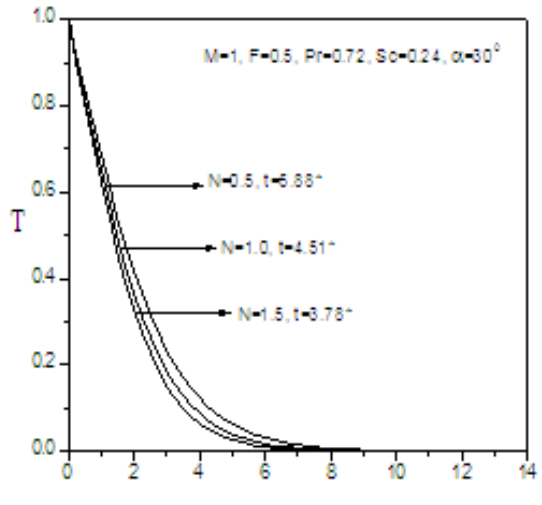

Fig 7 Steady state temperature for different values of *N* at X=1.0.

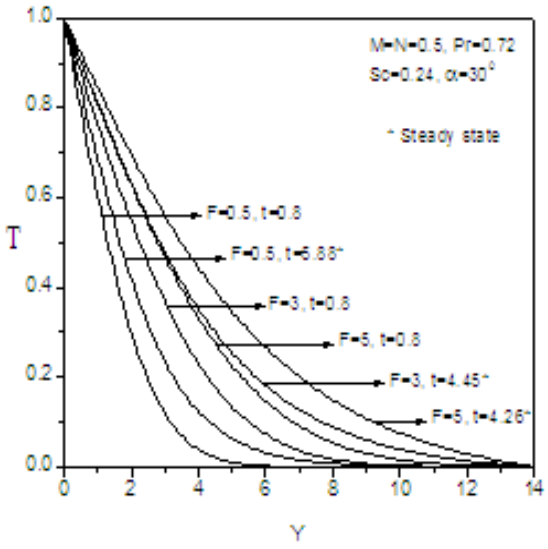

Fig 8 Transient temperature at X=1.0 for different values of *F*.

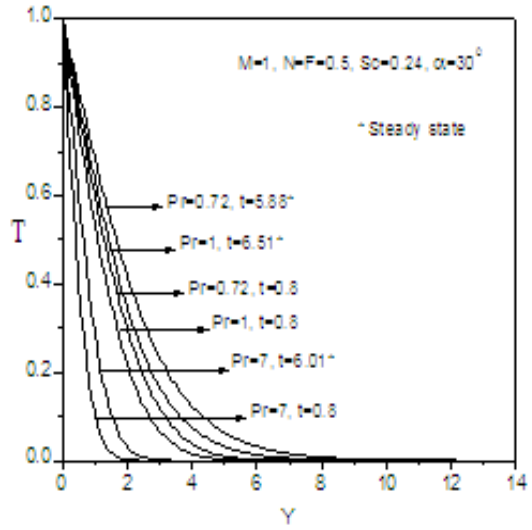

Fig 9 Transient temperature at X=1.0 for different values of *Pr*.

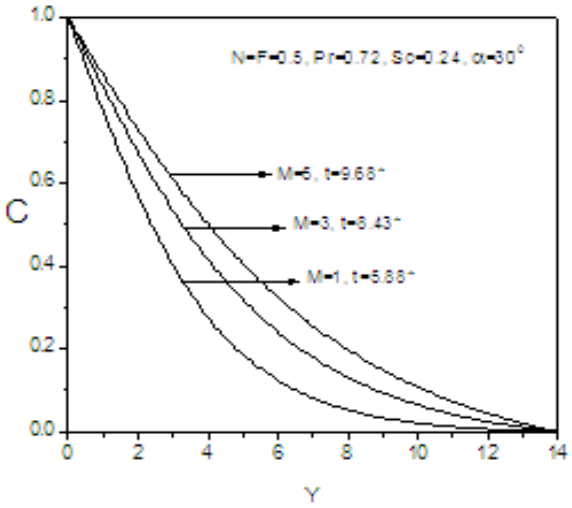

Fig 10 Steady state concentration for different values of *M* at X=1.0.

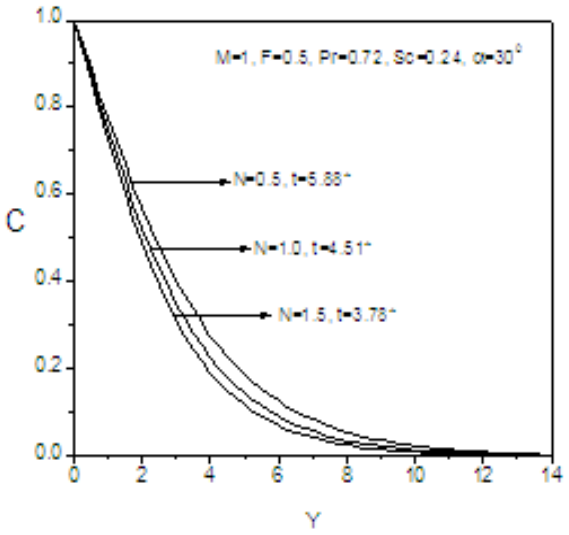

Fig 11 Steady state concentration for different values of *N* at X=1.0.

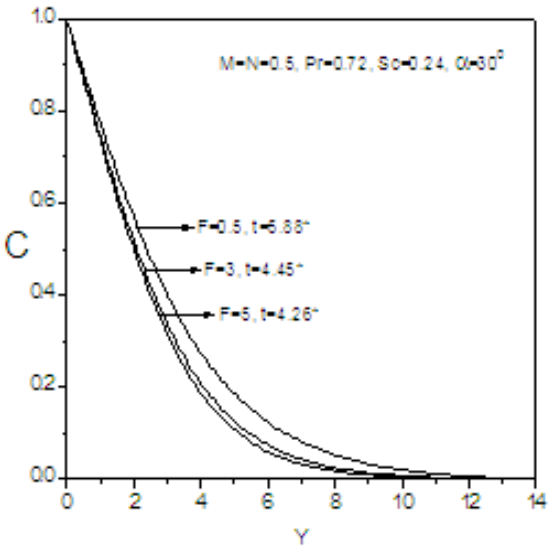

Fig 12 Steady state concentration for different values of *F* at X=1.0.

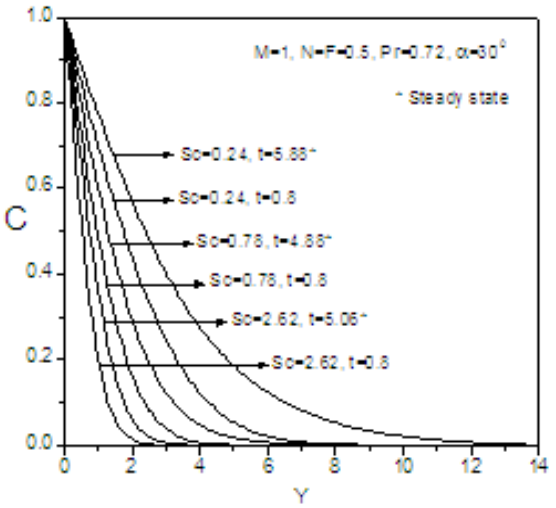

Fig 13 Transient concentration at X=1.0 for the different values of *Sc*.

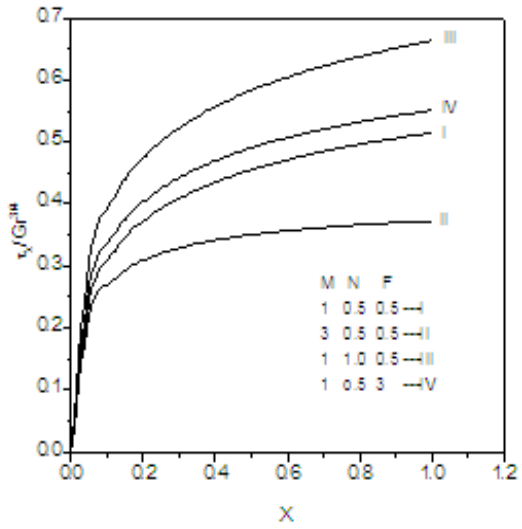

Fig 14 The effects of *M*, *N* and *F* on local skin friction.

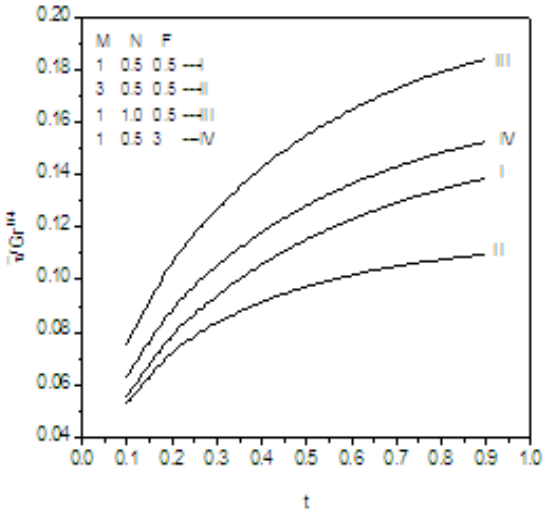

Fig 15 The effects of *M*, *N* and *F* on average skin friction.

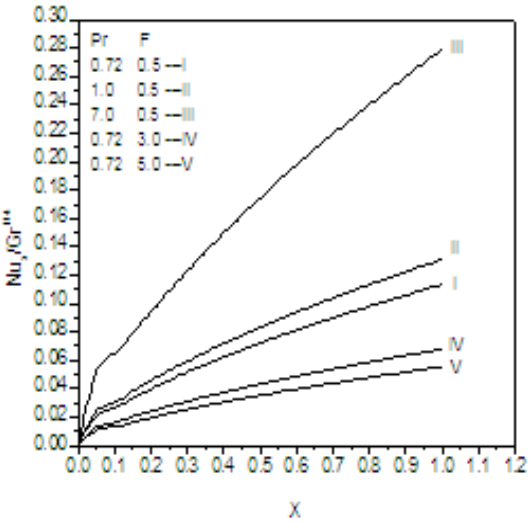

Fig 16 The effects of *Pr* and *F* on local Nusselt number.

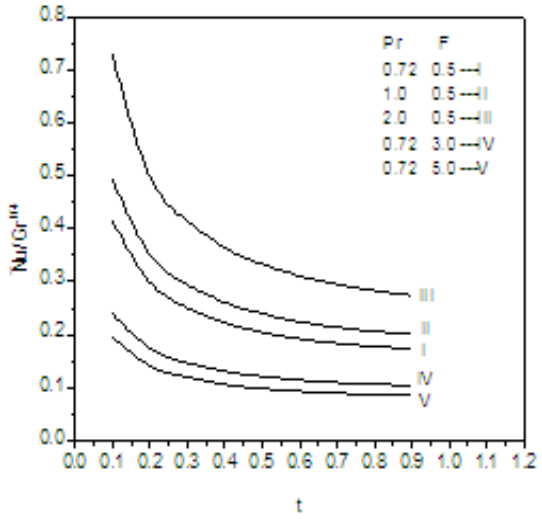

Fig 17 The effects of *Pr* and *F* on average Nusselt number.

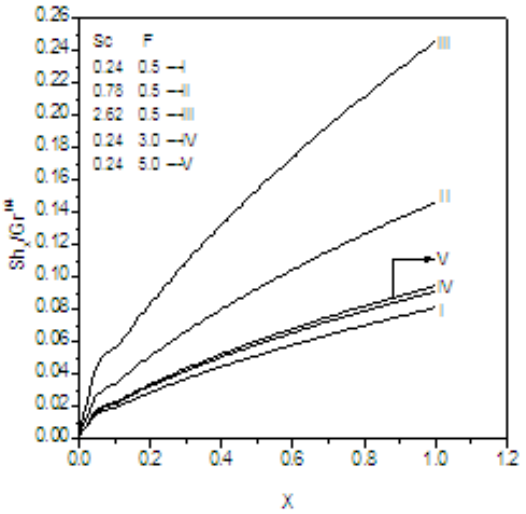

Fig 18 The effects of *Sc* and *F* on local Sherwood number.

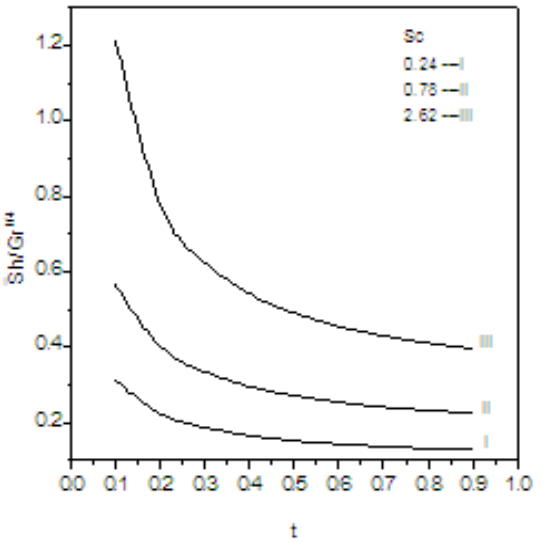

Fig 19 The effect of Schmidt number on average Sherwood number.

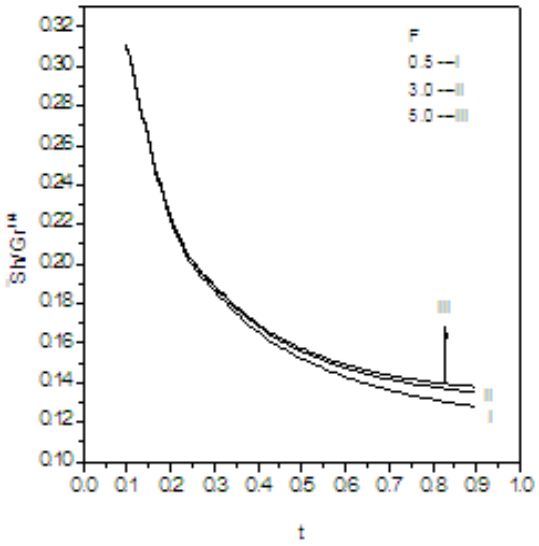

Fig 20 The effect of *R* on average Sherwood number.

REFERENCES

[1]. Callahan, G. D. and Marner, W.J., (1976), Transient free convection with mass transfer on an isothermal vertical flat plate, Int. J. Heat and Mass transfer, Vol.19, pp. 165-174.

[2]. Soundalgekar , V.M. and Ganesan, P., (1980), Transient free convection flow on a semi-infinite vertical plate with mass transfer, Reg. J. Energy Heat Mass Transfer, Vol.2, pp. 83-91.

[3]. Asma Begum, Abdul Maleque, Md., Ferdows, M., and Masahiro Ota, (2012), Finite Difference Solution of Natural Convection Flow over a Heated Plate with Different Inclination and Stability Analysis, Applied Mathematical Sciences, Vol.6, No.68, pp.3367-3379.

[4]. Callahan, G. D. and Marner, W. J. (1976), Int. J. Heat and Mass Trans., pp 149-165.

[5]. Soundalgekar, V. M., and Ganesan, P., (1985) Finite difference analysis of transient free convection with mass transfer on an isothermal vertical flat plate., Int. J. Engg Sci. 19, pp 757-770.

[6]. Marner, W. J. and Callahan, G. D., (1976), Int. J. Heat and Mass Trans., pp 19,165.

[7]. Chamkha, A. J., Rahim, A. and Khalid, A., (2001), Heat and Mass trans., Vol.37, pp.117.

[8]. Ganesan, P. and Palani, G., (2003), Free convection effects on the flow of water at 4ºC past a semi-infinite inclined plate, Heat and mass Transfer, Vol.39, pp.785-789.

[9]. Huges, W.F. and Young, F.J., (1966), The Electro-Magneto Dynamics of fluids, John wiley and sons, New York.

[10]. Raptis, A., (1986), Flow through a porous medium in the presence of magnetic field, Int. J.Energy. Res., Vol.10, pp. 97-101.

[11]. Helmy, K.A., (1998), MHD unsteady free convection flow past a vertical porous plate, ZAMM, Vol.78, pp. 255-270.

[12]. Elabashbeshy, E.M.A., (1997), Heat and Mass transfer along a vertical plate with variable surface temperature and concentration in the presence of the magnetic field, Int. J. Eng Sci., Vol.34, pp. 515- 522.

[13]. Cess, R.D., (1964), Radiation effects upon boundary layer flow of an absorbing gas, ASME. J. Heat Transfer, Vol.86c, pp.469-475.

[14]. Mosa, M.F., (1979), Radiative heat transfer in horizontal MHD channel flow with buoyancy effects and an axial temperature gradient, Ph.D. thesis, Mathematics Department, Bradford University, England, U.K,.

[15]. Nath, O., Ojha, S.N. and Takhar, H.S., (1991), A study of stellar point explosion in a radiative MHD medium, Astrophysics and Space Science, Vol.183, pp.135-145.

[16]. Takhar H.S., Gorla R.S.R. and Soundalgekar, V.M., (1996), Radiation effects on MHD free convection flow of a gas past a semi-infinite vertical plate, Int. J. Numer.Methods Heat Fluid Flow, Vol.6(2), pp77.

[17]. Gamal El-Din., Azzam, A., (2002), Radiation effects on the MHD mixed free-forced convection flow past a semi-infinite moving vertical plate for high temperature difference, Phys. Scripta, Vol.66, pp71.

[18]. Brewster, M.Q., (1992), Thermal radiative transfer and properties, John Wiley & Sons, New York.